

Coupled Modeling for Self Consistent Equilibrium Evolution Using the IPS Framework

M. Cianciosa¹, N. Isernia², G. Rubinacci², D. Terranova³, F. Villone²

¹ Oak Ridge National Laboratory, Oak Ridge, TN, United States

² Consorzio CREATE, DIETI, Universitá degli Studi di Napoli Federico II, Naples, Italy

³ Consorzio RFX, Padua, Italy

Due to the expense of ITER and the large energies involved, transient effects that could potentially damage first-wall and plasma-facing components must be avoided at all costs. Perturbations in the equilibrium result in induced currents in the conducting materials of the device. These eddy currents produce vacuum field errors that change the equilibrium. If not controlled, this feedback loop can result in an equilibrium colliding with the wall and disrupting. To avoid these damaging displacement events, ITER discharges need to be simulated first to understand potential catastrophic failures. Axisymmetric dynamic equilibrium codes like CREATE-NL+[1] can simulate the dynamic equilibrium under the influence of axisymmetric induced currents. However, port openings, reinforcement structures, blanket modules, and other features break axisymmetry. Accurately modeling these effects requires a fully 3D approach.

VMEC is a fully free boundary 3D equilibrium code that assumes closed nested flux surfaces[2]. Originally deployed for stellarators, VMEC has been used to model and reconstruct 3D effects in tokamaks[3]. VMEC minimizes the static force residuals

$$\vec{J} \times \vec{B} - \mu_0 \nabla P = 0 \quad (1)$$

to solve for the equilibrium state. Free boundary support is handled by minimizing the $\langle \vec{B} \cdot \vec{B} \rangle$ from the internal fields and external fields[4] at the boundary where

$$\vec{B}_{ext} = \vec{B}_{plasma} + \vec{B}_{coil}. \quad (2)$$

From a VMEC equilibrium solution, fields resulting from equilibrium plasma current can be

⁰Notice of Copyright This manuscript has been authored by UT-Battelle, LLC under Contract No. DE-AC05-00OR22725 with the U.S. Department of Energy. The United States Government retains and the publisher, by accepting the article for publication, acknowledges that the United States Government retains a non-exclusive, paid-up, irrevocable, world-wide license to publish or reproduce the published form of this manuscript, or allow others to do so, for United States Government purposes. The Department of Energy will provide public access to these results of federally sponsored research in accordance with the DOE Public Access Plan (<http://energy.gov/downloads/doe-public-access-plan>).

computed at the conductors using the Biot-Savart law

$$\vec{A} = \frac{\mu_0}{4\pi} \iiint \frac{\vec{J}(\vec{x}')}{|\vec{x} - \vec{x}'|} d\vec{x}' . \quad (3)$$

However, VMEC can only compute static equilibria. Given a fixed pressure and current profile VMEC solves the equilibrium state for that singular moment. To simulate time dynamics, multiple equilibria need to be computed from a time series of current and plasma profiles.

To model time dynamics, VMEC is coupled into a workflow using the Integrated Plasma Simulator (IPS)[5]. IPS is a python based framework for coupling codes that can utilize high-performance computing (HPC) resources. The IPS workflow sets the equilibrium profiles for the current time step. Executes VMEC then retrieves the solved equilibrium. The solution of the equilibrium is achieved through the V3FIT equilibrium reconstruction code[3] to ensure the solution remains within the bounds of the device. This time sequence of static equilibria must take into account the effects of eddy currents, which are related to the change in vector potential between subsequent time steps.

Faraday's law states that any time variation in a magnetic field will result in an induced current with a conducting material. Cariddi is a code that can compute the eddy current response to changes in the magnetic field using fully 3D geometry[6]

$$\vec{I}_{induced} = \vec{C}_1 \cdot \Delta \vec{A} + c . \quad (4)$$

where $\Delta \vec{A}$ is the change in the vector potential and c is a known term. Using the vector potential, as opposed to the magnetic field directly, ensures divergence free fields are retained. Eddy currents then produce a vacuum magnetic field response which can be computed via Biot-Savart integral, described by matrix Q

$$\vec{B}_{induced} = \vec{Q} \cdot \vec{K}_1 \cdot \Delta \vec{A} + d . \quad (5)$$

Initially, there are no eddy currents in the conducting structures. Finite resistance in these structures results in a decay of these currents that needs to be modeled as time advances. The induction and decay of induced currents can be discretized in time

$$\vec{I}_n = \vec{C}_1 \cdot (\vec{A}_n - \vec{A}_{n-1}) + \vec{C}_2 \cdot \vec{I}_{n-1} \quad (6)$$

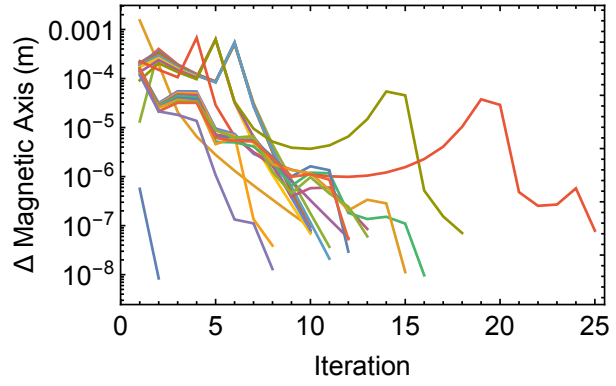


Figure 1: *Inner loop convergence of the magnetic axis.*

$$\vec{B}_n = \vec{K}_1 \cdot (\vec{A}_n - \vec{A}_{n-1}) + \vec{K}_2 \cdot \vec{I}_{n-1}. \quad (7)$$

Matrices $(\vec{C}_1, \vec{C}_2, \vec{K}_1, \vec{K}_2)$ encode all the physics of the eddy current response and 3D geometry of the conducting structures into a linear response.

At each time step, the workflow sets the current equilibrium profiles, solves the equilibrium, and computes the fields at the first wall surface. From the difference in these first wall fields, equations 6 and 7 compute the eddy currents that new vacuum field response. However, this does not result in a self-consistent equilibrium.

A second inner time loop is needed to converge the equilibrium to self consistent solution. From equation 7, the eddy current vacuum response is added to the vacuum fields of equations 2

$$\vec{B}_{ext} = \vec{B}_{plasma} + \vec{B}_{coil} + \vec{B}_{eddy}. \quad (8)$$

Each step in this inner loop takes the new vacuum fields with the eddy current contribution and computes a new equilibrium. This new equilibrium is used to update the eddy current vacuum fields. This cycle is repeated until a stable solution is reached.

A simple Picard iteration of the minor time step results in a numerically unstable growth of eddy current fields. Instead a damped iteration is employed that tries to minimize the change of the next iteration based on the previous. At each inner time step, the magnetic field is updated with a damping term α

$$\vec{B} = \vec{B}_{n-1} + \alpha \delta \vec{B}_n \quad (9)$$

At each iteration we seek to minimize

$$\left\| \vec{B}_{n-1} + \alpha \delta \vec{B}_n - \vec{K}_1 \cdot \vec{A} \left(\vec{B}_{n-1} + \alpha \delta \vec{B}_n \right) - \vec{d}_n \right\| \quad (10)$$

where $\vec{d}_n = -\vec{K}_1 \cdot \vec{A}_{n-1} + \vec{K}_2 \cdot \vec{I}_{n-1}$ and $\delta \vec{B}_n = \vec{K}_1 \cdot \vec{A}_n + \vec{d} - \vec{B}_{n-1}$. Under a linearization hypothesis, The minimum of equation 10 is found at

$$\alpha = \frac{\left(\delta \vec{B}_n - \vec{K}_1 \delta \vec{A}_n \right)^T \delta \vec{B}_n}{\left(\delta \vec{B}_n - \vec{K}_1 \delta \vec{A}_n \right)^T \left(\delta \vec{B}_n - \vec{K}_1 \delta \vec{A}_n \right)} \quad (11)$$

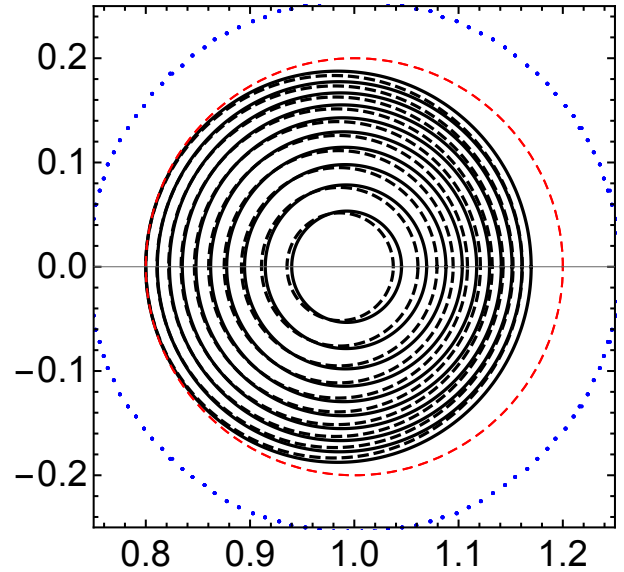


Figure 2: The equilibrium shifts to the left over the course of the simulation. The solid flux surfaces are the initial equilibrium and the dashed surfaces are the final.

is updated with a damping term α

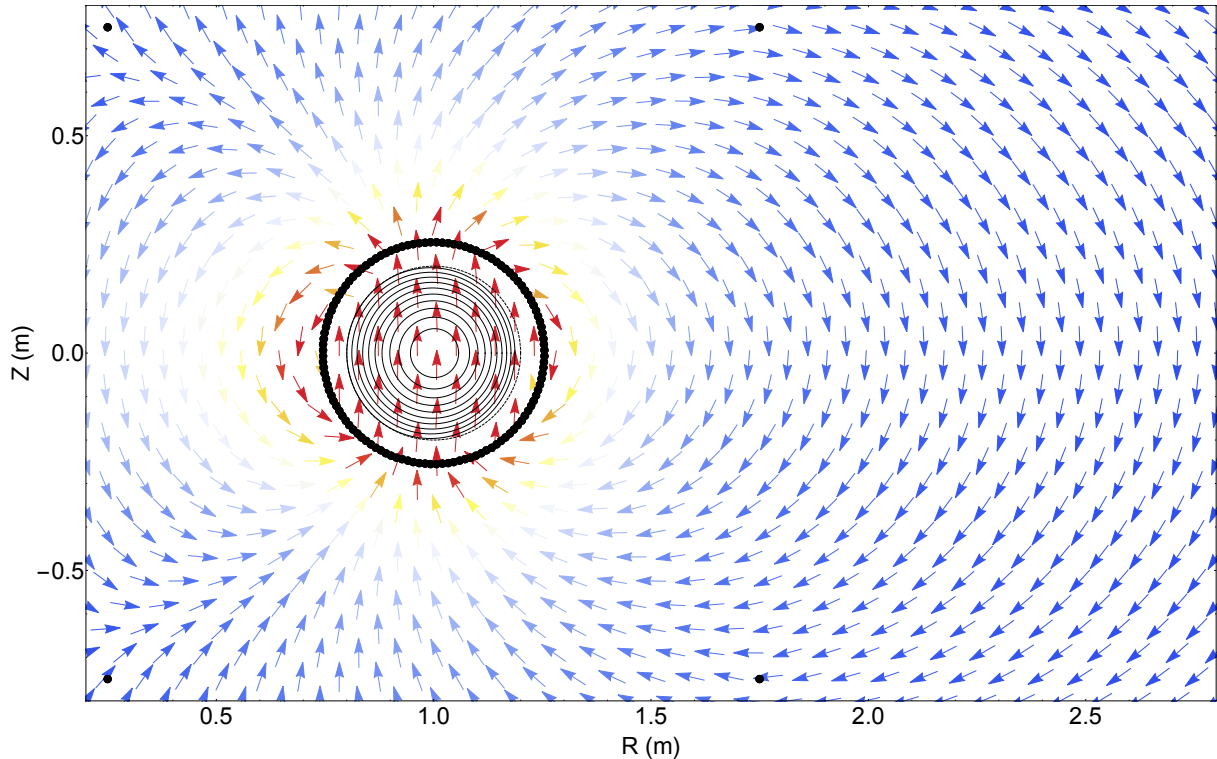


Figure 3: A leftward shift in plasma results in a vertical to stabilizing field.

where $\delta \vec{A}_n = \vec{A}(\vec{B}_{n-1} + \delta \vec{B}_n) - \vec{A}(\vec{B}_n)$. Using this scheme results in a sequence of configurations that converges to a stable equilibrium. Figure 1 shows the convergence of the change in the magnetic axis for each simulated time step.

This workflow was tested on a simplified circular cross-section tokamak configuration. Changes in the equilibrium profiles result in an inward shift of the equilibrium (Figure 2). The resulting eddy currents produce a vertical stabilizing field (Figure 3). Future work will apply this to realistic ITER configuration to model vertical displacement events (VDE) with comparison with evolutionary equilibrium codes like CarMa0NL[7].

References

- [1] R. Albanese, R. Ambrosino and M. Mattei, *Fusion Eng. Design* **96-97**, 664-667 (2015)
- [2] S.P. Hirshman and J.C. Whitson, *Phys. Fluids* **26**, 3553 (1983)
- [3] M. Cianciosa, A. Wingen, S.P. Hirshman, et. al., *Nucl. Fusion* **57** 076015 (2017)
- [4] S.P. Hirshman, W.I. van RIJ, P. Merkel, *Comp. Phys. Comm.* **43** 143-155 (1986)
- [5] W.R. Elwasif, D.E. Bernholdt, A.G. Shet, et. al., *18th Euromirco Conf. on Parallel, Distributed and Network-based Processing*, 419-427 (2010)
- [6] R. Albanese, G. Rubinacci, *IEE Proceedings A*, **135** 457-462 (1988)
- [7] F. Villone et al., *Plasma Phys. Control. Fusion*, **55** 095008 (2013)